

## MULTI-WIRE PROFILE MONITOR FOR J-PARC 3GEV RCS

S. Hiroki<sup>#</sup>, N. Hayashi, M. Kawase, F. Noda<sup>†</sup>, P. K. Saha, H. Sako, H. Takahashi, A. Ueno  
 JAEA, Tokai, Ibaraki 319-1195, Japan  
 Y. Arakida, S. Lee, T. Toyama, KEK, Tsukuba, Ibaraki 305-0801, Japan

### Abstract

A set of six multi-wire profile monitors (MWPMs) has been installed in the injection line and the successive H0 dump line of the RCS (Rapid Cycling Synchrotron), and contributed to the initial RCS commissioning for establishing an optimum injection orbit.

### INTRODUCTION

A layout of the injection line and H0 dump line is shown in Fig. 1, where large and complicated apparatuses such as magnets, foil units and beam monitors are installed in spatially limited areas. In the injection line, the H<sup>-</sup> beam from the Linac is exchanged to H<sup>+</sup> beam through the 1st foil and the H<sup>+</sup> beam is injected to the 3 GeV ring. The no exchanged H<sup>-</sup> and H<sup>0</sup> are converted to H<sup>+</sup> going through the 2nd and 3rd foils and entered to the H0 dump line. The bump magnet system synchronously merges the Linac H<sup>-</sup> beam into the 3 GeV ring H<sup>+</sup> beam [1]. However, the Insulated Gate Bipolar Transistor (IGBT) based power supply of the bump system generates a serious level of pulse noise, so we in particular concentrated on the pulse noise reduction work of the MWPM electronics.

MWPM is basically measured at lower than 1 % of the rated beam particle number ( $8.3 \times 10^{13}$ /pulse at 25 Hz) [2] and one pass mode. In an earlier MWPM design, the wire pitch was selected to 1 mm with a fixed frame position, considering the operational experience on the KEK PS [3]. However during the MWPM fabrication, the wire pitch was reconsidered, because the 1 mm pitch was too short to interfere with the neighbour wires by a capacitive coupling and a beam scattering, so it was resultantly expanded to more than 3 mm. In addition, the frame could be scanned at 0.1 mm pitch for use as a wire scanner.

### DESIGN AND FABRICATION

The MWPM2 to 5 were designed for the H<sup>-</sup> detection, whereas the MWPM6, 7 for the H<sup>+</sup> detection. The gold (Au) coated tungsten (W) wires were selected [3] for the H<sup>-</sup> beam detection by roughly evaluating a wire heating and an induced charge signal [4]. Specific properties of the W wire are:

Diameter	0.1 mm
Specific heat	0.15 J/(g·K)
Emissivity	0.05 and 0.1
(Considering 1 μm thickness Au coating)	

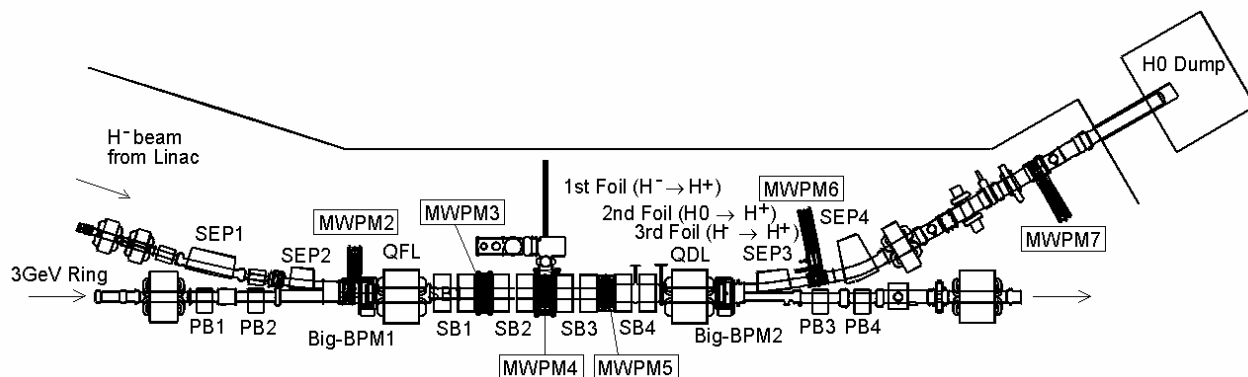


Figure 1: Layout of the RCS injection line and H0 dump line. The six MWPMs (MWPM2-7) were installed in the injection line and the H0 dump line. The MWPM1 installed in the ring was excluded. SEP: Septum magnet, QFL, QDL: Quadrupole magnets, PB: Paint bump magnet, SB: Shift bump magnet, Big-BPM: Beam position monitor.

In an initial RCS commissioning, it is important to establish a beam loss free orbit of the injection line as quickly as possible, so the MWPM has been selected for the injection beam monitor, because it is an interceptive device giving a reliable beam size and position, although a higher beam intensity destroys the wire, and a spatial resolution depends on the wire pitch. Therefore, the

The beam properties in the MWPM operation are:

Beam energy	181 MeV
Peak current	5 mA
Pulse width	35 μsec
Reputation rate	1 Hz

In the heating evaluation, the wire was assumed to a 0.1 mm square-cut and only thermal radiation heat loss ( $\sigma T^4$ ) was considered for simplification. In the H<sup>-</sup> injection, two separated 0.1 MeV electrons additionally heat the wire. When the beam radius is 2.8 mm (predicted rms beam at x-direction of MWPM2), the wire temperature is 1,000 K

<sup>#</sup>hiroki.seiji@jaea.go.jp  
<sup>†</sup>Present affiliation: Hitachi Ltd.

at 110sec for the emissivity of 0.01 as indicated in Fig. 2, which is far below the W melting point of 3643 K. Although the low emissivity of Au enhances the wire temperature, adsorption of residual gases to the wire will decrease.

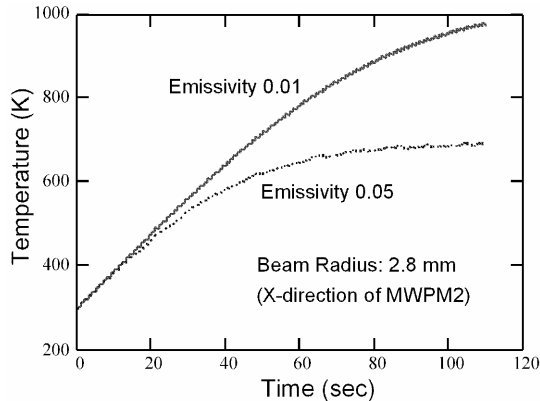


Figure 2: Estimated wire temperature vs. time at 1 Hz beam injection.

In addition, the induced charge signals are evaluated as a function of the beam radius as shown in Fig.3, where two separated electrons are trapped in the wire and the separated proton emits secondary electrons [5]. The secondary electron yield  $Y$  is denoted as

$$Y = \frac{P d_s}{E_k} \frac{dE}{dx}, \quad (1)$$

where  $P$  (0.5) is the probability of an electron escaping,  $d_s$  (1 nm) is the average depth of the secondary electron emission,  $E_k$  (25 eV) is the average kinetic energy lost by the incoming particle per ionization and  $dE/dx$  is the stopping power. The total induced charge ( $Q$ ) of  $-8,000$  pC is predicted for the 2.8 mm  $H^-$  beam, which gives the signal voltage of  $-2$  V ( $V=Q/C$ ) through the 40 m twisted pair cable (see Fig. 5,  $C \approx 4,000$  pF). However, only 0.02 V is calculated for the 16.2 mm radius  $H^+$  beam at the x-direction of MWPM6 ( $Q \approx 70$  pC of secondary electron in Fig. 3). A preliminary noise test on the bump magnets indicated a superposition of tens of mV pulse-noise, so in the MWPM6 and 7, the 0.1mm $\phi$  wire was replaced by a 1.0 mm width titan (Ti) foil of 10  $\mu$ m thickness [6] to increase the signal voltage.

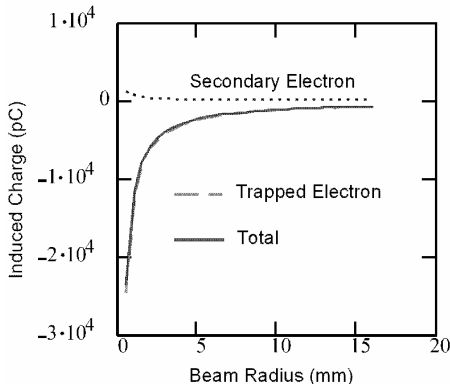


Figure 3: Induced charge signals vs. beam radius.

The MWPM2 wire sensor for the  $H^-$  beam is illustrated in Fig. 4. The 0.1mm $\phi$  wires were clamped to L shape small pin connectors pressed into holes of a ceramic wind frame for two directions (u: 8 wires and v: 28 wires with 17.7° tilt), which configured the actual u and v wire pitches of 9.5 mm and 2.9 mm, respectively. Both ends of the wire formed 1mm $\phi$  coil springs to apply a steady tension. In addition, the u and v directions wires were 7.4 mm apart for the beam direction. The frame could be scanned for the x direction. A combination of the 17.7° tilt wires and the precise scan function provided two step measurements, i.e. in the early stage a rough profile was obtained only at one shot, and a detailed profile was measured for typically 101 shots (10 mm scan at 0.1 mm interval) thereafter.

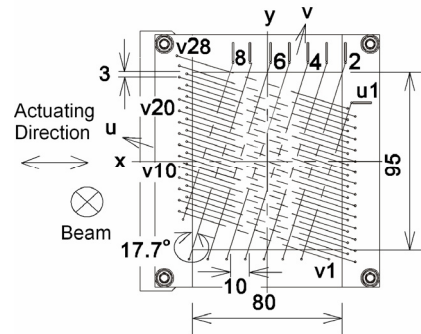


Figure 4: Wire sensor for MWPM2.

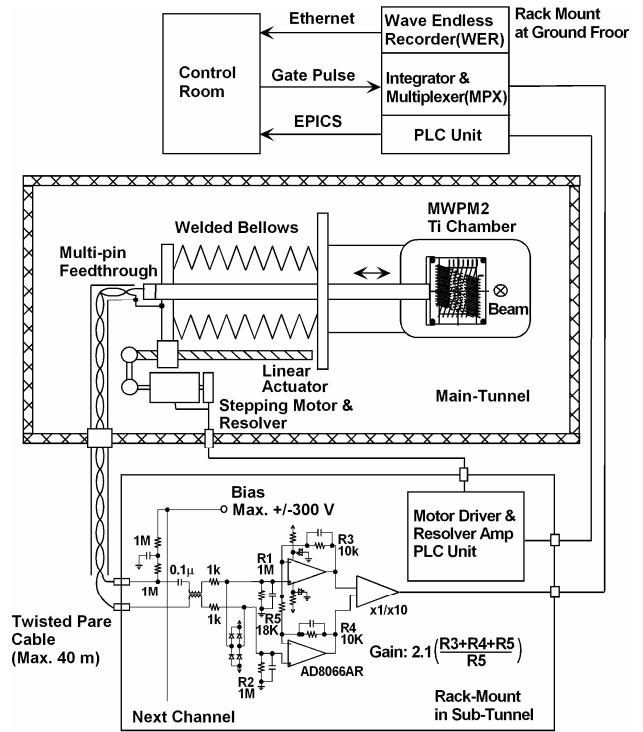


Figure 5: Overall configuration of MWPM2.

An overall configuration of MWPM2 is shown in Fig.5, where the wire sensor is installed in a rectangular Ti chamber of low activation material. An outgassing rate of the chamber was  $<10^{-8}$  Pa·m<sup>3</sup>/s per unit area, after 150 °C

and 24 hours baking. The cantilever sensor was externally linear actuated by a 5-phase stepping motor. The PEEK (poly-ether-ether-ke-ton) insulated coil windings and a special gear grease were used in the stepping motor and the resolver to enhance radiation tolerability. An origin of the sensor centre was estimated in the MWPM2 installation and alignment.

The beam induced charge signals were amplified by the instrumentation pre-amps located in a basement sub-tunnel at distances of 30-40 m from the wire sensor through the shielded twisted pair cables. The pre-amp signals were further transferred to the integrators for integrating a predetermined gate time and sequentially multiplexed (MPX) for 10 μs interval (Cable ≈150 m). The MPX output was digitized by the Wave Endless Recorder at the ground floor. The digitized profile was processed to the Gaussian fitting [7].

### EXPERIMENTAL RESULTS

On October 4, 2007, the first Linac beam was introduced to the RCS injection line, since then, steady beam experiments have been performed. An example of the MWPM2 pre-amp signal of CH4, equivalent of the u4 wire (see Fig. 4), is shown in Fig. 6, where the induced peak voltage of roughly 0.25 V is obtained. The 5 mA, 30 μs width beams of 110 shots were injected at 1 Hz, and the beam synchronous 50 μs gate pulse triggered the 0.1 mm step sensor scan for 10mm and each signal integration. Although the bump magnet induced pulse noises superimposed on the signal, they could effectively cancelled by the integrator due to the AC like noise.

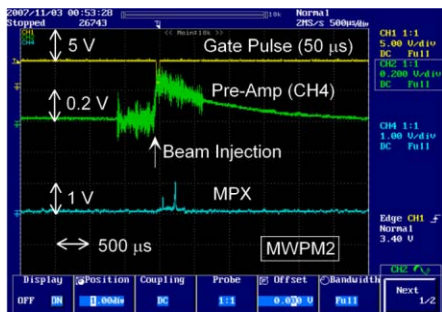


Figure 6: Example of MWPM2 pre-amp signal (Gain x1) and MPX output.

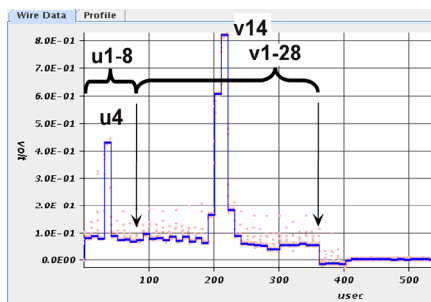


Figure 7: Digitized MPX output of MWPM2 in u-v plane.

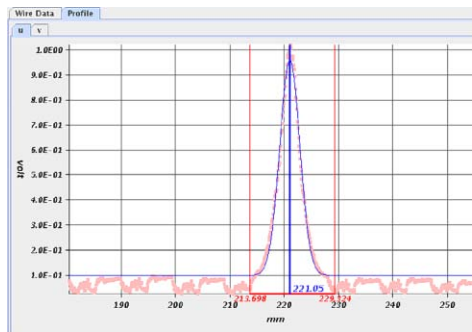


Figure 8: Gaussian fitting of MWPM2 wire data for u direction.

Figure 7 graphs the digitized MPX output at 1st shot of 110 shots, in which the integrated voltages are retrieved from the u1 to u8 wire related CH1-8 and the successive v1-28 at 10 μs intervals. The beam primarily hits the u4 and v14 wires and during the 10 mm sensor scan. The integrated voltages at 110 wire positions were averaged. Figure 8 plots an example of the MWPM2 beam profile with the Gaussian fitting as a function of the u-plane position. The beam core in x-y plane was calculated as (231.2 mm, 2.6 mm) from the ring orbit center. Almost same results were obtained in the MWPM3-7.

### CONCLUSIONS

The MWPMs were designed and installed in the RCS injection area. A wire heating and an induced charge level were evaluated, and the 0.1 mmφ W wire (for H<sup>-</sup>) and the 1 mm width Ti foil (for H<sup>+</sup>) were selected for the sensor materials. The MWPMs were successfully used in the initial RCS commissioning.

### REFERENCES

- [1] T. Takayanagi et al., “Design of the injection bump system of the 3-GeV RCS in J-PARC”, IEEE Trans. Appl. Superconductivity 16 (2006) 1358.
- [2] Y.Yamazaki, et al., “Approach to a Very High Intensity Beam at J-PARC”, Proc. HB2006, Tsukuba, May 2006, MOAP01.
- [3] T. Adachi, et al., “Estimation of the Particle Density in Transverse Phase Space Using a Multi-Wire Profile Monitor”, EPAC’98, Stockholm, June 1998, p. 1479.
- [4] R. E. Shafer, “Performance of a Tungsten-Wire Profile Scanner in the SNS Superconducting Linac”, 30/April/00, SNS NOTE SNS-Tech 104050200-TD0001-R00.
- [5] E.J.Sternglass, “Theory of Secondary Electron Emission by High-Speed Ions”, Phys. Rev. 108 (1957) 1.
- [6] S. Kopp, et al., “Segmented Foil SEM Grids at Fermilab”, Fermilab-Conf-05-092-AD (2005).
- [7] H. Sako, et al., “An Application for Beam Profile Reconstruction with Multi-Wire Profile Monitors at J-PARC RCS”, TUPC092, this conference.